A High-Speed Parallel Robot for Scara Motions

Sébastien Krut[1] ♣, Vincent Nabat ♦, Olivier Company ♣, François Pierrot ♣
<krut, nabat, company, pierrot>@lirmm.fr

(♣) LIRMM, UMR 5506 CNRS – Université Montpellier II
161, rue Ada, 34392 Montpellier cedex 5, France

(♦) FATRONIK
Polígono Ibaitarte, 1- 20870 Elgoibar, Spain

***Abstract* — This paper introduces a new 4 degree-of-freedom parallel robot. It presents its architecture inspired by FlexPicker, an ABB machine based on the Delta architecture, while overcoming its drawbacks. This paper exposes the way to get the geometrical models, and particularly the forward position relationship which can be obtained in a closed form. In a third part, a detailed study of the robot singularities is made by taking into account the not-so-classic internal singularities. Design conditions are obtained for isostatic and over-constrained cases. The robot optimization and its workspace are finally presented.**

***Keywords* — Scara motions; PKM; Pick-and-place.**

I. INTRODUCTION

The idea of parallel mechanisms resorting to a non-rigid moving platform which includes passive joints and dedicated to Scara motions has been introduced recently and a few academic prototypes have already demonstrated the effectiveness of this principle [3] [7]. Indeed, the 4 *dof* (degrees of freedom) of Scara motions are well adapted to pick-and-place tasks: 3 translations to carry an object from one point to another, plus one rotation about a given axis in world coordinates for the orientation. Robots inspired from Delta [1] architecture encountered a real commercial success achieving this task, because of their high dynamics. This is due to the lightweight (actuators are fixed on the base) parallel (having closed kinematics chains) design. However, the ***R***UPUR kinematic chain (*R*: Revolute, *U*: Universal, *P*:Prismatic, bold letter stands for actuated joint)) that transmits the rotational motion from a revolute actuator fixed on the frame to the effector (see Figure 1) may become a weak point. This is particularly true for Delta with huge workspace or, even more, with linear Delta.

Most of recent researches in that field have proposed different designs for obtaining Scara motions; some of them are parallel mechanisms, like Kanuk [2] or H4 [3], some others have non-fully-parallel designs [4]. Other four-dof parallel mechanisms have been studied in the past, but they are dedicated to different applications such as Koevermans' flight simulator [5] and Reboulet's four-dof wrist [6]. Even more recently, a machine with a moving platform including passive prismatic joints and a "Translation-to-Rotation" transformation system has been introduced [7]; in the later paper it was shown that for a very specific design ((i) four linear motors in the same plane and aligned on the same direction, (ii) a three-part moving platform) it was possible to get a realistic practical design and very simple kinematics model in closed form for both Inverse and Forward problems.

The aim of this paper is to go one step further and to show that is indeed possible to obtain a design which compares directly with commercially available Delta-based robots (*e.g.* the FlexPicker, an ABB Robotics equipment) in terms of technology, workspace, performance while avoiding the ***R***UPUR kinematic chain.

To do so, we have designed a prototype of a machine we called I4R by resorting to several components from FlexPicker. In this paper, this prototype is described and the way to achieve the desired rotation is discussed. Then, geometrical models are derived. A nice feature for this robot is that the forward geometrical model can be written in a closed form. Afterward, a kinematic modeling able to witness to all the singularities of the robot is established: this is based on a detailed modeling of the so-called "spatial parallelograms" which are described here for what they really are (two *SS* chains). It shows up the geometrical condition that must be validated in order to get the desired motions. Two different modeling are given: one is isostatic and the other over-constrained. At the end, the optimization of the machine is explained and the workspace is presented.

Figure 1. ABB Robotics FlexPicker

[1] Currently with the JRL, AIST-CNRS Joint Lab, Tsukuba

II. DESCRIPTION OF THE PROTOTYPE

The practical design is extremely simple thanks to the forearms and spatial parallelograms taken from the FlexPicker (see Figure 2, left hand side).

The main difference with the FlexPicker results in the use of 4 parallelograms instead of 3. Furthermore, instead of being rigid, the moving platform is articulated and does not require the kinematic chain transmitting the rotational motion to the effector. It is composed of two different parts (while the machine in [7] utilizes a three-part moving platform) linked together by a primatic guide, plus a pulley-cable system which transforms the relative translation of both parts into the desired rotation (see Figure 2, right hand side).

It gives a workspace similar to FlexPicker's one – a 1-meter radius, 0.2-meter high cylinder – but overcomes the problems due to the effector's rotation. The brushless revolute actuators are associated to gear units with very low backlash (<1'). Moving parts are intended to be as light as possible: forearms and parallelograms are carbon fiber parts (from ABB Robotics), while the traveling plate is made of aluminum. The expected performances for this robot are: 100 [m/s^2] acceleration and 10 [m/s] velocity (*Note: It is too early to guarantee that such performances will be reached, even though our first tests are encouraging*).

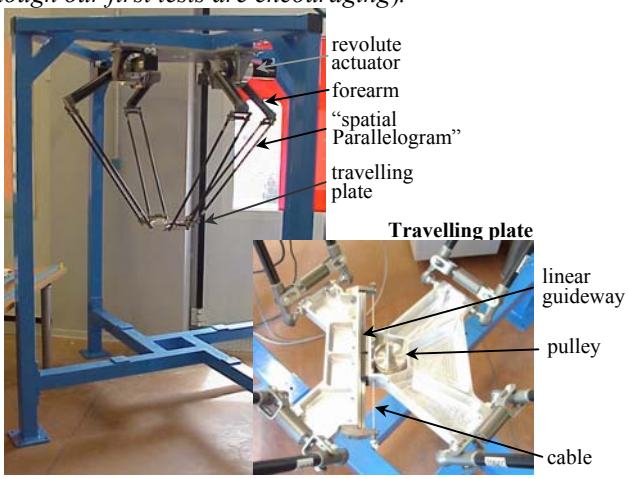

Figure 2. Pictures of the first I4R prototype

III. MODELING

In Figure 3, a joint-and-loop graph is depicted: gray boxes represent actuated joints, white boxes passive joints. Underlined letter stands for a joint equipped with sensors. Circles express a coupling between two joints. It is worth noting that this mechanism is, on one hand *under-constrained* (as for many Delta-like designs, each rod between two *S* joints can rotate about its own axis) and on the other hand, *over-constrained* (a Grübler analysis would show one degree of constraint: this will be further analyzed in section IV). Figure 4 depicts the whole geometry of the mechanism.

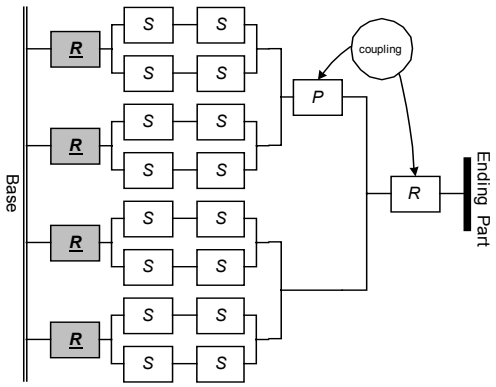

Figure 3. I4R's joint-and-loop graph

* $\boldsymbol{x} = [x \quad y \quad z \quad \theta]^T$ is the generalized operational vector.

* $\boldsymbol{q} = [q_i]$ is the generalized joint vector. q_i are the joint coordinates (angles measured in planes $(\mathrm{P}_i, \vec{e}_z, \vec{u}_i)$ starting from $\vec{e}_z$).

* P_i[2], $i \in \{1,2,3,4\}$, represent the positions of the actuators:

$$\boldsymbol{P}_1 = [-e \quad -d \quad 0]^T, \boldsymbol{P}_2 = [e \quad -d \quad 0]^T, \tag{1}$$

$$\boldsymbol{P}_3 = [-e \quad d \quad 0]^T, \boldsymbol{P}_4 = [e \quad d \quad 0]^T, \tag{2}$$

* $\vec{u}_i$ characterizes the orientation of the forearms:

$$\boldsymbol{u}_i = [\cos(\alpha_i) \quad \sin(\alpha_i) \quad 0]^T, \; i \in \{1,2,3,4\}, \tag{3}$$

where α_i are angles measured about $\vec{e}_z$ relatively to $\vec{e}_x$.

* A_i is the geometrical point located in the middle of A_{i1} and A_{i2} representing the spherical joints centers:

$$\boldsymbol{A}_i = \boldsymbol{P}_i + \boldsymbol{L}_i, \; i \in \{1,2,3,4\} \tag{4}$$

with:

$$\boldsymbol{L}_i = [L\sin(q_i)\cos(\alpha_i) \quad L\sin(q_i)\sin(\alpha_i) \quad L\cos(q_i)]^T, \tag{5}$$

where: L is the length of the bars.

* B_i is the geometrical point situated in the middle of B_{i1} and B_{i2} representing the center of the spherical joints between the forearms and the moving platform:

$$\boldsymbol{B}_i = \boldsymbol{D} + k_i\,\theta\,\boldsymbol{v}_1 + \boldsymbol{E}_i, \; i \in \{1,2,3,4\}, \tag{6}$$

with:
$$k_1 = k_2 = R \text{ and } k_3 = k_4 = 0, \tag{7}$$

$$\boldsymbol{D} = [x \quad y \quad z]^T, \tag{8}$$

$$\boldsymbol{E}_1 = [-E \quad -D \quad 0]^T, \boldsymbol{E}_2 = [E \quad -D \quad 0]^T, \tag{9}$$

$$\boldsymbol{E}_3 = [-E \quad D \quad 0]^T, \boldsymbol{E}_4 = [E \quad D \quad 0]^T, \tag{10}$$

[2] Each geometrical vector $\vec{u}$ will be associated to a column vector $\boldsymbol{u}$ expressed in the canonic base $\mathcal{B} = (\vec{e}_x, \vec{e}_y, \vec{e}_z)$. Moreover, column vector $\boldsymbol{P}$ will represent geometrical point P in frame $\Re = \langle \mathrm{O}, \mathcal{B} \rangle$.

$$\boldsymbol{v}_1 = \boldsymbol{e}_x \tag{11}$$

($\boldsymbol{v}_1$ characterizes the direction of the guide and R is the radius of the pulley: $t = R\theta$.)

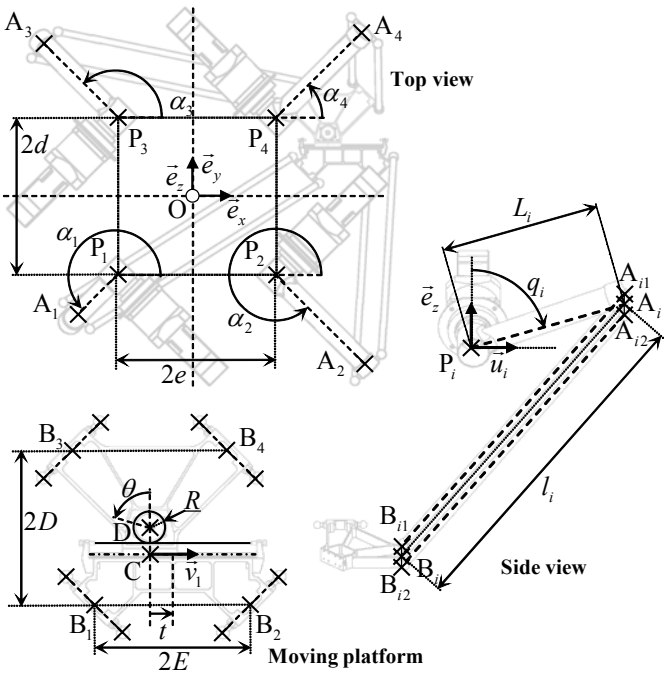

Figure 4. Geometrical modeling of the I4R structure

A. Relation between $\boldsymbol{x}$ and $\boldsymbol{q}$

1) Inverse position relationship

As it is usual for most parallel robots, the inverse position relationship is easy to derive from the following equality:

$$\|\boldsymbol{l}_i\| = l\,,\ i \in \{1,2,3,4\} \tag{12}$$

where $\boldsymbol{l}_i$ is the vector joining A_i to B_i ($\boldsymbol{l}_i = \boldsymbol{A}_i - \boldsymbol{B}_i$)

For this robot the resolution is derived for rotational motors as in [14] and leads to:

$$M_i \cos(q_i) + N_i \sin(q_i) = G_i\,,\ i \in \{1,2,3,4\} \tag{13}$$

where: $$M_i = 2L(\boldsymbol{B}_i\boldsymbol{P}_i.\boldsymbol{e}_z)\,,\ N_i = 2L(\boldsymbol{B}_i\boldsymbol{P}_i.\boldsymbol{u}_i)\,, \tag{14}$$

$$G_i = l^2 + \|\boldsymbol{B}_i\boldsymbol{P}_i\|^2 - L^2\,,\ \boldsymbol{B}_i\boldsymbol{P}_i = \boldsymbol{P}_i - \boldsymbol{B}_i\,. \tag{15}$$

($\boldsymbol{B}_i$ is given by relation (6) when knowing the operational coordinate vector. "$.$" represents a dot product).

Making the classical change of variable:

$$t_i = \tan(q_i/2)\,, \tag{16}$$

leads to a second degree polynomial equation. Once solved, only the root corresponding to the realistic posture is kept, and the joint coordinates can be written as follow:

$$q_i = 2\tan^{-1}\left(\frac{-b_i + \sqrt{b_i^2 - 4a_ic_i}}{2a_i}\right),\quad i \in \{1,2,3,4\} \tag{17}$$

with a_i, b_i and c_i the polynomial coefficients:

$$a_i = G_i + M_i\,,\ b_i = -2N_i \text{ and } c_i = G_i - M_i\,. \tag{18}$$

2) Forward position relationship

In a general manner, it is always preferable to have the forward position relationship written in a closed form. Such a model can be derived for the I4R robot. The main reason is that operational parameters can be decoupled: y and z parameters can be derived independently of x and θ. Furthermore, y and z can be computed as the intersection of two ellipses.

a) Decoupling operational variables

In fact, developing relations (12) about the operational parameters leads to the following 4-equation system:

$$(x + k_i\theta)^2 + 2a_i(x + k_i\theta) + y^2 + 2b_i\,y + z^2 + 2c_i\,z + d_i = 0\,, \tag{19}$$

where: $$a_i = \boldsymbol{A}_i\boldsymbol{E}_i.\boldsymbol{e}_x\,,\ b_i = \boldsymbol{A}_i\boldsymbol{E}_i.\boldsymbol{e}_y\,,\ c_i = \boldsymbol{A}_i\boldsymbol{E}_i.\boldsymbol{e}_z\,, \tag{20}$$

$$d_i = \boldsymbol{A}_i\boldsymbol{E}_i^{\,2} - l_i^2\,,\ \boldsymbol{A}_i\boldsymbol{E}_i = \boldsymbol{E}_i - \boldsymbol{A}_i\,,\ i \in \{1,2,3,4\}\,. \tag{21}$$

($\boldsymbol{A}_i$ is given by relation (4) and (5) while knowing the joint parameters).

By subtracting the two first equations of this system and the two last, the following equalities are derived:

$$\begin{cases} x + R\theta = \dfrac{(b_2 - b_1)}{(a_1 - a_2)}y + \dfrac{(c_2 - c_1)}{(a_1 - a_2)}z + \dfrac{(d_2 - d_1)}{(a_1 - a_2)} & (22) \\ x = \dfrac{(b_4 - b_3)}{(a_3 - a_4)}y + \dfrac{(c_4 - c_3)}{(a_3 - a_4)}z + \dfrac{(d_4 - d_3)}{(a_3 - a_4)} & (23) \end{cases}$$

When merging those results into 1st and 3rd equations of system (19), the following system composed of two quadrics depending only on y and z is derived:

$$\alpha_i\,y^2 + \beta_i\,z^2 + \chi_i\,y\,z + \delta_i\,y + \varepsilon_i\,z + \phi_i = 0\,,\ i \in \{1,2\} \tag{24}$$

where α_i, β_i, χ_i, δ_i, ε_i and ϕ_i depend on the joint coordinates:

$$\alpha_i = \frac{(b_k - b_j)^2}{(a_j - a_k)^2} + 1 \quad \beta_i = \frac{(c_k - c_j)^2}{(a_j - a_k)^2} + 1 \quad \chi_i = \frac{(b_k - b_j)(c_k - c_j)}{(a_j - a_k)^2} \tag{25}$$

$$\delta_i = 2\frac{(d_k - d_j)(b_k - b_j)}{(a_j - a_k)^2} + 2a_j\frac{(b_k - b_j)}{(a_j - a_k)} + 2b_j \tag{26}$$

$$\varepsilon_i = 2\frac{(d_k - d_j)(c_k - c_j)}{(a_j - a_k)^2} + 2a_j\frac{(c_k - c_j)}{(a_j - a_k)} + 2c_j \tag{27}$$

$$\phi_i = 2\frac{(d_k - d_j)^2}{(a_j - a_k)^2} + 2a_j\frac{(d_k - d_j)}{(a_j - a_k)} + d_j \tag{28}$$

with $(i,j,k) \in \{(1,1,2),(2,3,4)\}$.

b) Computing z as the intersection of two ellipses

Once the operational parameters are decoupled, the focus is given to the resolution of parameters y and z. They correspond to the intersection of two ellipses as it can be observed on Figure 5.

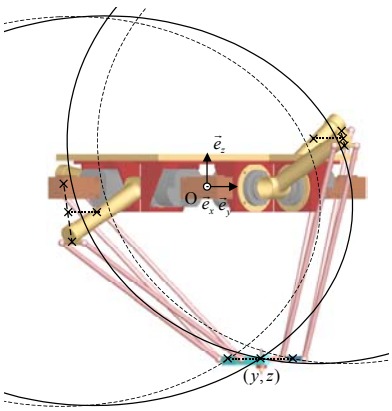

Figure 5. Intersecting ellipses

The algebraic solutions of this problem are known [18] and consist in resolving the following 4th degree polynomial equation in z :

$$P(z) = u_4 z^4 + u_3 z^3 + u_2 z^2 + u_1 z + u_0 \quad (29)$$

The above polynomial is obtained with the change of variables:

$$u_0 = v_2 v_{10} - v_4^2,\ u_1 = v_0 v_{10} + v_2 (v_7 + v_9) - 2 v_3 v_4, \quad (30)$$

$$u_2 = v_0 (v_7 + v_9) + v_2 (v_6 - v_8) - v_3^2 - 2 v_1 v_4 \quad (31)$$

$$u_3 = v_0 (v_6 - v_8) + 2 v_2 v_5 - 2 v_1 v_3,\ u_4 = v_0 v_5 - v_1^2, \quad (32)$$

with: $$v_0 = \alpha_1 \chi_2 - \alpha_2 \chi_1,\ v_1 = \alpha_1 \beta_2 - \alpha_2 \beta_1, \quad (33)$$

$$v_2 = \alpha_1 \delta_2 - \alpha_2 \delta_1,\ v_3 = \alpha_1 \varepsilon_2 - \alpha_2 \varepsilon_1,\ v_4 = \alpha_1 \phi_2 - \alpha_2 \phi_1, \quad (34)$$

$$v_5 = \chi_1 \beta_2 - \chi_2 \beta_1,\ v_6 = \chi_1 \varepsilon_2 - \chi_2 \varepsilon_1,\ v_7 = \chi_1 \phi_2 - \chi_2 \phi_1, \quad (35)$$

$$v_8 = \beta_1 \delta_2 - \beta_2 \delta_1,\ v_9 = \delta_1 \varepsilon_2 - \delta_2 \varepsilon_1,\ v_{10} = \delta_1 \phi_2 - \delta_2 \phi_1. \quad (36)$$

The method proposed by Cardan and Ferrari [19] gives the real roots of polynomial equation (29) in a closed form: it consists in solving in a first step a 3rd degree polynomial equation. This method presented numerical instabilities and a more robust formulation was chosen [20][21][22]: it consisted in finding solutions either real or complex.

Practically, equation (29) as only two real solutions, that are both represented on Figure 5. So, choosing the proper solution for z consists in keeping only the lowest real root (decided from geometrical considerations).

c) Computing all other operational variables

Once z is determined, the aim is to compute y by using system (24). Whether than preferring one of the two equations, it is better to subtract both equations in order to eliminate the y^2 term. It leads to the following expression:

$$y = \frac{(\alpha_1 \beta_2 - \alpha_2 \beta_1) z^2 + (\alpha_1 \varepsilon_2 - \alpha_2 \varepsilon_1) z + (\alpha_1 \phi_2 - \alpha_2 \phi_1)}{(\alpha_2 \chi_1 - \alpha_1 \chi_2) z + (\alpha_2 \delta_1 - \alpha_1 \delta_2)} \quad (37)$$

At last, the determination of x is obtained with (23), and θ is calculated by solving system (22) :

$$\theta = \left(\frac{(b_2 - b_1)}{(a_1 - a_2)} y + \frac{(c_2 - c_1)}{(a_1 - a_2)} z + \frac{(d_2 - d_1)}{(a_1 - a_2)} - x \right) \Big/ R \quad (38)$$

IV. SINGULARITY ANALYSIS

Singularities analysis is often based on analysis of the standard Jacobean matrices $\boldsymbol{J}_x$ and $\boldsymbol{J}_q$ representing the input-output velocity relationship:

$$\boldsymbol{J}_q \dot{\boldsymbol{q}} = \boldsymbol{J}_x \dot{\boldsymbol{x}}, \quad (39)$$

where $\dot{\boldsymbol{q}}$ and $\dot{\boldsymbol{x}}$ are respectively the joint velocity vector and the operational velocity vector.

But other kind of singularities can occur [8]. To enlighten them, a deeper analysis is required. At first, we will recall the fact that "spatial parallelograms" can be seen in two different ways, and that we consider here the realistic case where spherical joints are modeled as 3-dof joints and not 2-dof joints. Then, two types of modeling will be given: one suggesting that the linear guide is a cylindrical joint (isostatic modeling), and another assuming that it is a prismatic joint (over-constrained modeling). In both case, geometrical constraints, which must be fulfilled to get rid of internal singularities, will be derived.

A. Preliminary remark

According to Hervé's notations [23] for displacements subgroups, $\{T\}$ stands for the subgroup of spatial translations and $\{X(\mathbf{u})\}$ stands for the subgroup of Schoenflies displacements (or Scara motion), where $\mathbf{u}$ is a unitary vector collinear to the rotation's axis. If a closed loop mechanism is composed of two chains producing Schoenflies displacements with $\mathbf{v} \neq \mathbf{u}$, then:

$$\{X(\mathbf{u})\} \cap \{X(\mathbf{v})\} = \{T\} \quad (1)$$

that is to say that such a mechanism will produce only three translations. The case of machines with ***R***$R(RR)_2R$ chains (Figure 6-a) is easily handled with such a technique since those chains correspond to Schoenflies subgroup.

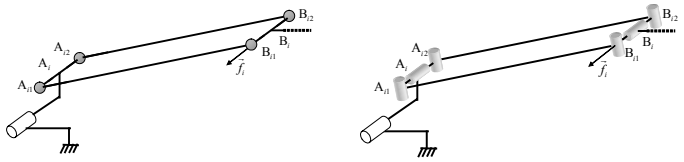

(a) $\boldsymbol{P}(SS)_2$ (b) $\underline{\boldsymbol{P}}R(RR)_2R$

Figure 6. Two ways to model the "spatial parallelograms".

The case of machines with $\underline{\boldsymbol{R}}(SS)_2$ chains (Figure 6-b) is more complex: each chain provides 5 *dof*, 3T-2R, and does not correspond to a group. Indeed it is possible that the union ($\cup$)

of two 3T-2R chains generates a 3T-3R motion. The following sub-sections consider precisely this type of $\underline{\boldsymbol{R}}(SS)_2$ chains.

B. Isostatic modelling

Here, the prismatic guide is represented by a *cylindrical joint* offering one degree of freedom in translation and one degree of freedom in rotation along the same axis. Such an hypothesis offers: (i) a number of internal dof consistent with a Grübler analysis (no internal constraint), (ii) a model of prismatic joint with very low torsional stiffness.

On the one hand, a 4-dof subset made of the actuators can be observed. On the other hand, an 8-dof traveling plate can be found: 3 for positioning, 3 for orientating, and 2 considering inter-part mobilities (the linear guide is represented by a 2-dof cylindrical joint). Single bars equipped with spherical joints separate both subsets. Each implies that the distance between their extremities is invariant:

$$\left\| \boldsymbol{l}_{ij} \right\| = l \ , \ i \in \{1,2,3,4\} \ , \ j \in \{1,2\} \ , \tag{40}$$

where $\boldsymbol{l}_{ij}$ is the vector joining A_{ij} to B_{ij} ($\boldsymbol{l}_{ij} = \boldsymbol{A}_{ij} - \boldsymbol{B}_{ij}$).

Deriving this relation leads to the equiprojectivity of velocities of the extremities of each rod:

$$\boldsymbol{v}_{\mathrm{A}_{ij}} . \boldsymbol{l}_{ij} = \boldsymbol{v}_{\mathrm{B}_{ij}} . \boldsymbol{l}_{ij} \ , \ i \in \{1,2,3,4\} \ , \ j \in \{1,2\} \ , \tag{41}$$

where $\boldsymbol{v}_{\mathrm{A}_{ij}}$ (respectively $\boldsymbol{v}_{\mathrm{B}_{ij}}$) represents the velocity of point A_{ij} (B_{ij}) relatively to the ground.

As a consequence, a linear system representing the whole kinematic of the mechanism can be derived when writing the equiprojectivity relations for the 8 rods:

$$\begin{bmatrix} \boldsymbol{r}_1.\boldsymbol{l}_{11} & 0 & 0 & 0 \\ \boldsymbol{r}_1.\boldsymbol{l}_{12} & 0 & 0 & 0 \\ 0 & \boldsymbol{r}_2.\boldsymbol{l}_{21} & 0 & 0 \\ 0 & \boldsymbol{r}_2.\boldsymbol{l}_{22} & 0 & 0 \\ 0 & 0 & \boldsymbol{r}_3.\boldsymbol{l}_{31} & 0 \\ 0 & 0 & \boldsymbol{r}_3.\boldsymbol{l}_{32} & 0 \\ 0 & 0 & 0 & \boldsymbol{r}_4.\boldsymbol{l}_{41} \\ 0 & 0 & 0 & \boldsymbol{r}_4.\boldsymbol{l}_{42} \end{bmatrix} \begin{bmatrix} \dot{q}_1 \\ \dot{q}_2 \\ \dot{q}_3 \\ \dot{q}_4 \end{bmatrix} =$$

$$\begin{bmatrix} \boldsymbol{l}_{11}{}^T & R\boldsymbol{v}_1.\boldsymbol{l}_{11} & [\boldsymbol{e}_{11}\times\boldsymbol{l}_{11}]^T & (\boldsymbol{v}_1\times\boldsymbol{d}_{11}).\boldsymbol{l}_{11} \\ \boldsymbol{l}_{12}{}^T & R\boldsymbol{v}_1.\boldsymbol{l}_{12} & [\boldsymbol{e}_{12}\times\boldsymbol{l}_{12}]^T & (\boldsymbol{v}_1\times\boldsymbol{d}_{12}).\boldsymbol{l}_{12} \\ \boldsymbol{l}_{21}{}^T & R\boldsymbol{v}_1.\boldsymbol{l}_{21} & [\boldsymbol{e}_{21}\times\boldsymbol{l}_{21}]^T & (\boldsymbol{v}_1\times\boldsymbol{d}_{21}).\boldsymbol{l}_{21} \\ \boldsymbol{l}_{22}{}^T & R\boldsymbol{v}_1.\boldsymbol{l}_{22} & [\boldsymbol{e}_{22}\times\boldsymbol{l}_{22}]^T & (\boldsymbol{v}_1\times\boldsymbol{d}_{22}).\boldsymbol{l}_{22} \\ \boldsymbol{l}_{31}{}^T & 0 & [\boldsymbol{e}_{31}\times\boldsymbol{l}_{31}]^T & 0 \\ \boldsymbol{l}_{32}{}^T & 0 & [\boldsymbol{e}_{32}\times\boldsymbol{l}_{32}]^T & 0 \\ \boldsymbol{l}_{41}{}^T & 0 & [\boldsymbol{e}_{41}\times\boldsymbol{l}_{41}]^T & 0 \\ \boldsymbol{l}_{42}{}^T & 0 & [\boldsymbol{e}_{42}\times\boldsymbol{l}_{42}]^T & 0 \end{bmatrix} \begin{bmatrix} \dot{x} \\ \dot{y} \\ \dot{z} \\ \dot{\theta} \\ \omega_x \\ \omega_y \\ \omega_z \\ \dot{\varepsilon} \end{bmatrix} . \tag{42}$$

Where

"$\times$" represents the cross product

$\boldsymbol{r}_i$ is a vector tangent to the trajectory of points A_i, A_{i1} and A_{i2} . It verifies $\left\| \boldsymbol{r}_i \right\| = L$

$\boldsymbol{e}_{ij}$ is the vector joining D to B_{ij}

$\boldsymbol{d}_{ij}$ the vector joining the end point C to B_{ij}

ω_x, ω_y and ω_z are angular velocities of half moving platform {3-4} (upper part in Figure 4) relatively to the ground

$\dot{\varepsilon}$ the angular velocity of half traveling plate {1-2} (lower part) relatively to traveling plate's part 3-4 about $\boldsymbol{v}_1$.

Next step of the method consists in doing elementary operations on this system (which do not affect the rank of the system) to end up with the following system:

$$\begin{bmatrix} \boldsymbol{J}_q \\ \boldsymbol{0} \end{bmatrix} \dot{\boldsymbol{q}} = \begin{bmatrix} \boldsymbol{J}_x & \boldsymbol{J}_{int}^x \\ \boldsymbol{0} & \boldsymbol{J}_{int} \end{bmatrix} \begin{bmatrix} \dot{\boldsymbol{x}} \\ \boldsymbol{v}_{int} \end{bmatrix} \tag{43}$$

where $\boldsymbol{J}_{int}$ and $\boldsymbol{J}_{int}^x$ are 4×4 matrices and $\boldsymbol{v}_{int}$ is a velocity vector. This system has the particularity of being triangular by blocs. In this particular case, multiplying both parts of the system with the following invertible matrix:

$$\boldsymbol{M} = \begin{bmatrix} \frac{1}{2} & \frac{1}{2} & 0 & 0 & 0 & 0 & 0 & 0 \\ 0 & 0 & \frac{1}{2} & \frac{1}{2} & 0 & 0 & 0 & 0 \\ 0 & 0 & 0 & 0 & \frac{1}{2} & \frac{1}{2} & 0 & 0 \\ 0 & 0 & 0 & 0 & 0 & 0 & \frac{1}{2} & \frac{1}{2} \\ 1 & -1 & 0 & 0 & 0 & 0 & 0 & 0 \\ 0 & 0 & 1 & -1 & 0 & 0 & 0 & 0 \\ 0 & 0 & 0 & 0 & 1 & -1 & 0 & 0 \\ 0 & 0 & 0 & 0 & 0 & 0 & 1 & -1 \end{bmatrix} \quad (\det(\boldsymbol{M}) = 1) \tag{44}$$

and taking into account the fact that rods $i1$ and $i2$ are parallel, in working situation, leads to such a system. The results are:

$$\boldsymbol{J}_q = \begin{bmatrix} \boldsymbol{r}_1.\boldsymbol{l}_1 & 0 & 0 & 0 \\ 0 & \boldsymbol{r}_2.\boldsymbol{l}_2 & 0 & 0 \\ 0 & 0 & \boldsymbol{r}_3.\boldsymbol{l}_3 & 0 \\ 0 & 0 & 0 & \boldsymbol{r}_4.\boldsymbol{l}_4 \end{bmatrix} , \ \boldsymbol{J}_x = \begin{bmatrix} \boldsymbol{l}_1^T & R\boldsymbol{v}_1.\boldsymbol{l}_1 \\ \boldsymbol{l}_2^T & R\boldsymbol{v}_1.\boldsymbol{l}_2 \\ \boldsymbol{l}_3^T & 0 \\ \boldsymbol{l}_4^T & 0 \end{bmatrix} , \tag{45}$$

$$\boldsymbol{J}_{int}^x = \begin{bmatrix} [\boldsymbol{e}_1\times\boldsymbol{l}_1]^T & (\boldsymbol{v}_1\times\boldsymbol{d}_1).\boldsymbol{l}_1 \\ [\boldsymbol{e}_2\times\boldsymbol{l}_2]^T & (\boldsymbol{v}_1\times\boldsymbol{d}_2).\boldsymbol{l}_2 \\ [\boldsymbol{e}_3\times\boldsymbol{l}_3]^T & 0 \\ [\boldsymbol{e}_4\times\boldsymbol{l}_4]^T & 0 \end{bmatrix} , \ \boldsymbol{J}_{int} = \begin{bmatrix} [\boldsymbol{f}_1\times\boldsymbol{l}_1]^T & (\boldsymbol{v}_1\times\boldsymbol{f}_1).\boldsymbol{l}_1 \\ [\boldsymbol{f}_2\times\boldsymbol{l}_2]^T & (\boldsymbol{v}_1\times\boldsymbol{f}_2).\boldsymbol{l}_2 \\ [\boldsymbol{f}_3\times\boldsymbol{l}_3]^T & 0 \\ [\boldsymbol{f}_4\times\boldsymbol{l}_4]^T & 0 \end{bmatrix} , \tag{46}$$

and:

$$\boldsymbol{v}_{int} = \begin{bmatrix} \omega_x & \omega_y & \omega_z & \dot{\varepsilon} \end{bmatrix}^T \tag{47}$$

($\boldsymbol{e}_i$ is the vector joining D to B_i, $\boldsymbol{d}_i$ the one linking C to B_i, $\boldsymbol{f}_i$ is the vector linking B_{i1} to B_{i2} : $\boldsymbol{f}_i = \boldsymbol{e}_{i2} - \boldsymbol{e}_{i1}$.)

$\boldsymbol{J}_{int}$ will witness of – what we call – "internal singularities". In fact, if $\boldsymbol{J}_{int}$ is not singular, (43) implies that:

$$\boldsymbol{v}_{int} = \boldsymbol{0} \tag{48}$$

which means that half-travelling plate {3-4} keeps always the same orientation ($\omega_x = \omega_y = \omega_z = 0$) and it is the same for part {1-2} while $\dot{\varepsilon} = 0$.

Furthermore, relation:

$$\boldsymbol{J}_q \dot{\boldsymbol{q}} = \boldsymbol{J}_x \dot{\boldsymbol{x}} + \boldsymbol{J}_{int}^x \boldsymbol{v}_{int} . \tag{49}$$

derived from (43) falls into the usual velocity relationship (39).

Verifying $\boldsymbol{J}_{int}$ is not singular can be done by computing its determinant.

It leads to the particular following relationship:

$$\left(\left((\boldsymbol{f}_1\times\boldsymbol{l}_1)\times(\boldsymbol{f}_2\times\boldsymbol{l}_2)\right)\times\left((\boldsymbol{f}_3\times\boldsymbol{l}_3)\times(\boldsymbol{f}_4\times\boldsymbol{l}_4)\right)\right).\boldsymbol{e}_x \neq 0 \quad (50)$$

By verifying that this relation is always true in the whole workspace we can guarantee that no "internal" singularity occurs. For other type of singularities, usual Jacobean matrices need to be studied: $\boldsymbol{J}_q$ will enlighten "under-mobilities" and $\boldsymbol{J}_x$, "over-mobilities" [14].

C. *Over-constrained modelling*

This modeling considers the linear guide as a pure, one-dof, prismatic joint. It implies that the traveling plate is a subset with only 7 dof, and system (42) must be rewritten without considering terms associated to $\dot{\varepsilon}$. As a consequence, $\boldsymbol{J}_{int}$ and $\boldsymbol{J}_{int}^{x}$ are 4×3 matrixes:

$$\boldsymbol{J}_{int}^{x}=\begin{bmatrix}[\boldsymbol{e}_1\times\boldsymbol{l}_1]^T\\ [\boldsymbol{e}_2\times\boldsymbol{l}_2]^T\\ [\boldsymbol{e}_3\times\boldsymbol{l}_3]^T\\ [\boldsymbol{e}_4\times\boldsymbol{l}_4]^T\end{bmatrix},\ \boldsymbol{J}_{int}=\begin{bmatrix}[\boldsymbol{f}_1\times\boldsymbol{l}_1]^T\\ [\boldsymbol{f}_2\times\boldsymbol{l}_2]^T\\ [\boldsymbol{f}_3\times\boldsymbol{l}_3]^T\\ [\boldsymbol{f}_4\times\boldsymbol{l}_4]^T\end{bmatrix}. \quad (51)$$

The fact that system (42) gets over-determined (more equations than unknowns) reveals the over-constraint of the mechanism. To make sure the mechanism doesn't show "internal" singularities, we must guarantee that $\boldsymbol{J}_{int}$ is always of full rank ($\mathrm{rank}(\boldsymbol{J}_{int})=3$). Considering the symmetrical role of the 4 spatial parallelograms, we obtain the mathematical relation revealing "internal" singularities by developing arbitrary one of the four 3×3 determinant D_{ijk} of this matrix:

$$D_{ijk}=\det\left(\begin{bmatrix}[\boldsymbol{f}_i\times\boldsymbol{l}_i]^T\\ [\boldsymbol{f}_j\times\boldsymbol{l}_j]^T\\ [\boldsymbol{f}_k\times\boldsymbol{l}_k]^T\end{bmatrix}\right) \quad (52)$$

$$D_{ijk}=\left((\boldsymbol{l}_i\times\boldsymbol{l}_j).\boldsymbol{f}_i\right)\left((\boldsymbol{f}_j\times\boldsymbol{f}_k).\boldsymbol{l}_k\right)-\left((\boldsymbol{f}_i\times\boldsymbol{f}_j).\boldsymbol{l}_i\right)\left((\boldsymbol{l}_j\times\boldsymbol{l}_k).\boldsymbol{f}_k\right) \quad (53)$$

for $(i,j,k)\in\{(1,2,3),(1,2,4),(1,3,4),(2,3,4)\}$.

V. Optimization and Workspace

The parameters chosen for the prototype are:

$$\alpha_1=225° \quad \alpha_2=315° \quad \alpha_3=135° \quad \alpha_4=45° \quad (54)$$

$$D=E \quad d=e \quad (55)$$

which give the machine a symmetrical aspect.
Length of forearms and single rods measured on the parts taken from the FlexPicker robot are:

$$l=800\text{ mm} \quad L=351\text{ mm} \quad (56)$$

The goal of the optimization is to determinate the geometrical parameters of the robot. D and E were chosen as little as possible in order to obtain a compact travelling plate, and parameters d and e were optimized in order to minimize the following function:

$$\max\left(\mathrm{cond}\left(\boldsymbol{J}_m\boldsymbol{W}\right)\right) \quad (57)$$

inside the cylindrical workspace, such as:

$$\sqrt{x^2+y^2}\le 0{,}5\text{ m} \quad (58)$$

$$z\in[z_0-0{,}1\text{ m},\ z_0+0{,}1\text{ m}] \quad (59)$$

$$\theta\in[-180°,+180°] \quad (60)$$

$\boldsymbol{W}$ represents the weight matrix defined by:

$$\boldsymbol{W}=\begin{bmatrix}1&0&0&0\\0&1&0&0\\0&0&1&0\\0&0&0&\frac{1}{R}\end{bmatrix} \quad (61)$$

and z_0 the average altitude of the workspace (its value is calculated by optimization). The method used for this optimization is to calculate the function (57) for a set of geometrical configurations. The one which minimized the best (57) were chosen. The results are:

$$D=E=142\text{ mm},\ d=e=300\text{ mm} \text{ and } z_0=-530\text{ mm} \quad (62)$$

The workspace obtained for a weighted conditioning lower then 8 is given in Figure 7.
The pulley radius R has been chosen in order to obtain a complete revolution of the actuator for a 120 mm stroke of the prismatic joint. Thus:

$$R=21\text{ mm} \quad (63)$$

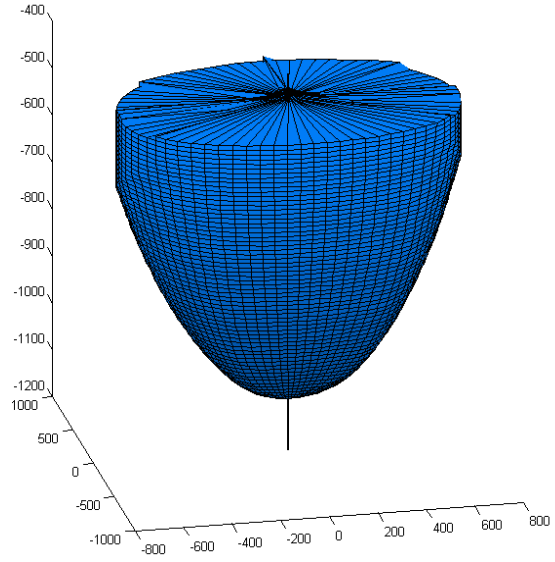

Figure 7. Workspace estimation $\mathrm{cond}(\boldsymbol{J}_m\boldsymbol{W})<8$

VI. CONCLUSION

This paper has introduced a new parallel mechanism inspired by the Delta architecture, while overcoming its drawbacks due to the kinematic chain that transmits the rotational motion. Indeed, the I4R uses 4 parallelograms and its articulated traveling plate allows the orientation of the effector. This new robot has been studied in details.

The calculation of geometrical models which are both obtained in a close way. Moreover, the study of singularities, using kinematic model, establishes geometrical conditions for an isostatic modeling and an over-constrained one. At least, the architecture has been optimized and the workspace taking into account the conditioning has been drawn.

The control of this robot is, to date, very simple (linear independent joint control) and will be improved in the future by using, for example, a dynamic control.

Acknowledgements. The help and support of Torgny Brogardh, from ABB Robotics Research Department, have really been appreciated.

VII. REFERENCES

[1] R. Clavel, "Une nouvelle structure de manipulateur parallèle pour la robotique légère", APII, 23(6), 1985, pp. 371-386.

[2] Rolland L., "The Manta and the Kanuk: Novel 4 dof parallel mechanism for industrial handling", in Proc. of ASME Dynamic Systems and Control Division IMECE'99 Conference, Nashville, USA, November 14-19, 1999, vol. 67, pp 831-844.

[3] Pierrot F., Company O., "H4: a new family of 4-dof parallel robots", in Proc of IEEE/ASME International Conference on Advanced Intelligent Mechatronics, Atlanta, Georgia, USA, September 19-22, 1999, pp. 508-513.

[4] Angeles J., Morozov A., Navarro O., "A novel manipulator architecture for the production of SCARA motions", in Proc. IEEE International Conference on Robotics and Automation, San Francisco, April 24-28, 2000, pp. 2370-2375.

[5] Koevermans W.P. et al., "Design and performance of the four dof motion system of the NLR research flight simulator", in Proc. of AGARD Conf., No 198, Flight Simulation, La Haye, 20-23 October 1975, pp. 17-1/17-11.

[6] Reboulet C. et al, "Rapport d'avancement projet VAP", thème 7, phase 3. Rapport de Recherche 7743, CNES/DERA, January 1991.

[7] Krut S., Company O., Benoit M., Ota H. and Pierrot F., "I4: A new parallel mechanism for Scara motions", in Proc. of IEEE ICRA: Int. Conf. on Robotics and Automation, Taipei, Taiwan, September 14-19, 2003.

[8] Zlatanov D., Fenton R.G., and Benhabib B., "Identification and classification of the singular configurations of mechanisms", Mechanism and Machine Theory, Vol. 33, No. 6, pp. 743-760, August 1998.

[9] Hervé J.M., "The Lie group of rigid body displacements, a fundamental tool for mechanism design", Mechanism and Machine Theory, Vol. 34, 1999, pp. 719-730.

[10] Furuya N., Soma K., Chin E., Makino, "Research and development of selective compliance assembly robot arm. II. Hardware and software of SCARA controller", Journal of the Japan Society of Precision Engineering/Seimitsu Kogaku Kaishi, Vol. 49, n°7, 1983, pp. 835-841.

[11] Pierrot F., Dauchez P. and Fournier A., "Fast parallel robots", Journal of Robotic Systems, 8(6), 1991, pp. 829-840.

[12] Hesselbach J., Plitea N., Frindt M., et Kusiek A., "A new parallel mechanism to use for cutting convex glass panels", in ARK, Strobl, June 29-July 4, 1998, pp. 165-174.

[13] Tanev T.K., "Forward displacement analysis of a three legged four-degree-of-freedom parallel manipulator", in ARK, Strobl, June 29-July 4, 1998, pp. 147-154.

[14] Merlet J.-P. and Pierrot F., "Modélisation des robots parallèles", in Analyse et modélisation des robots manipulateurs, Lavoisier, ISBN 2-7462-0300-6, 2001, pp. 93-144.

[15] Hervé J.M., "Analyse structurelle des mécanismes par groupes de déplacements", Mechanism and Machine Theory, Vol. 13, 1978, pp. 437-450.

[16] Company O., Pierrot F., "A new 3T-1R parallel robot", in Proc. of 9th International Conference on Advanced Robotics, Tokyo, Japan, October 25-27, 1999, pp. 557-562.

[17] Pierrot F., Marquet F., Company O., Gil T., "H4 parallel robot: modeling, design and preliminary experiments", in Proc. of IEEE Int. Conf. On Robotics and Automation, Seoul, Korea, May 2001.

[18] Eberly D., "Intersection of Ellipses", Magic Software Inc., 6006 Meadow Run Court, Chapel Hill, NC 27516, USA.

[19] Candido G., « Le risoluzioni della equazione di quarto grado (Ferrari-Eulero-Lagrange) », *Period. Mat.*, Vol. 4, No. 21, pp. 88-106, 1941.

[20] Durand E., Solution numérique des équations algébriques, Masson, Paris, 1960.

[21] Démidovitch B. and Maron I., Éléments de calcul numérique, Mir, Moscow, 1979.

[22] Mineur H., Technique de calcul numérique, Dunod, Paris, 1966.

[23] Hervé J.M., "The Lie group of rigid body displacements, a fundamental tool for mechanism design", *Mechanism and Machine Theory*, Vol. 34, 1999, pp. 719-730.